EVOLUTIONARY ALGORITHMS APPLIED TO LOW-THRUST FORMATION FLYING TRAJECTORY OPTIMIZATION

Jing Li[(1)], **Xiao-ning Xi**[(2)]
[(1)] *College of Aerospace Science and Technology, National University of Defense Technology, 410073 Changsha, China, +86 731 84576436, li0243268@sina.com*
[(2)] *College of Aerospace Science and Technology, National University of Defense Technology, 410073 Changsha, China, +86 731 84575397, xilily0704@126.com*

Abstract: *This paper investigates the application of evolutionary algorithms (EAs) for the fuel-optimal low-thrust formation flying trajectory optimization (FFTO) under the two control direction constraints based on the Clohessy-Wiltshire equations. First, by applying the Pontryagin's maximum principle, the first-order necessary optimality conditions are derived, which allow for using the initial costates to parameterize the FFTO problem. The search space of the initial costates is determined by enlarging the initial costates of the associated optimal impulsive trajectory. A penalty method is adopted by the EAs to find the optimal solution that satisfies the equality constraints presented in the shooting function. To settle the control discontinuity when propagating the trajectories, an integrator equipped with events detection technique is adopted to automatically determine the switching times according to the switching function. Finally, numerical examples are given to illustrate the performance of the method.*

Keywords: *Formation Flying, Evolutionary algorithms, Low-thrust Trajectory Optimization, Impulsive Optimal Trajectory, Two Thruster Configurations.*

1. Introduction

Formation flying is defined as a set of more than one satellite in which any of the satellite dynamic states are coupled through a common control law [1, 2]. It has been identified as an enabling technology for many future space missions, such as distributed aperature radar, virtual co-observation and stereo-imaging platforms for space science, and Earth observing, et al. The functionality of a single complex satellite can be distributed between a cluster of smaller closely satellites flying in formation. It enables the enhanced mission through the increase resolution of scientific observations, improve flexibility and redundancy, be real-time reconfigurable, adapt to highly dynamic demands, and lower life cycle costs. In an environment in which refueling is not possible and it is necessary to reduce the overall weight of the formation satellites, optimization of the fuel consumption can greatly influence the operational life of the formation. For this reason, low-thrust propulsion is becoming quite popular as it is characterized by a high value of specific impulse, allowing a reduction of the amount of propellant needed for the optimal trajectory control [3].

In general, numerical optimization methods can be classified as deterministic or heuristic methods. Deterministic methods are gradient-based methods, which assume the continuity and differentiability of the objective function to be minimized and can be further divided into direct methods and indirect methods [4, 5]. Direct methods transcribe the optimal control problem into a parameter optimization problem, which is solved by using optimization techniques. Direct methods are supposed to be more robust, but with a relatively low precision. Indirect methods use Pontryagin's maximum principle (PMP) to derive the first-order optimality conditions of the optimal control problem, which lead to a two-point boundary-value problem (TPBVP) that is solved by means of shooting methods [4]. Indirect methods have a higher precision but require the addition of the costates and their governing equations. Meanwhile, costates are non-physical quantities, it is very nonintuitive to estimate [4, 6]. If poorly provided, the resulting trajectories may be so wild that the intervening variables often exceed the numerical range of the computer [4, 6]. Betts [4] gave an excellent survey of the direct methods and indirect methods for trajectory optimization. Deterministic methods are gradient based optimization methods; they are local in nature and can search only the convex neighborhood around the initial guess. Therefore, the optimal solution gained is very sensitive to the initial guess and require the identification of a suitable first attempt solution in the region of convergence, which is unknown a priori and is strongly problem-dependent.

In the last decade, the heuristics methods, also referred to as evolutionary algorithms (EAs), have been successfully applied in aerospace applications. EAs are numerical optimizers that determine an optimal set of discrete parameters that has been used to parameterize the problem solution. The most popular class of these techniques is represented by genetic algorithms (GAs) [7], differential evolution (DE) algorithms [8, 9], and particle swarm optimization (PSO) algorithms [10, 11], et al. The general intent of the EAs is to improve over the pure grid or enumerative search. EAs have two principal advantages over all of the deterministic methods that 1) they require no initial "guess" of the solution (only the search space of the unknown decision variables are needed) and 2) they are more likely than other deterministic methods to locate a global minimum in the search space rather than be attracted to a local minimum. EAs are better suited to the optimization of impulsive trajectories, which can be described by a limited number of variables. Bessette and Spencer [12] employed the PSO for impulsive interplanetary trajectory optimization. Sentinella and Casalino [13] based on the GA, DE, and PSO, and run the three optimizers in parallel to optimize the multiple-impulse rendezvous trajectories and Earth-to-Mars round trip missions. Pontani and Conway [14] applied the PSO to impulsive orbital transfers.

For low-thrust trajectory optimization, the large number of variables required to describe the trajectory with sufficient accuracy makes the use of EAs for this kind of optimization problem less attractive. Recently, a number of papers focus on using EAs for low-thrust trajectory optimization [15-19]. To apply the EAs in searching for the low-thrust global optimal trajectories, a common way is adopting certain methods to parameterize the control profile, such as the B-splines [5, 18, 19] or polynomial function [17]. In Ref. [15], a time-optimal low-thrust trajectory is found by GA, where the thrust-pointing angle in each segment of the trajectory is assumed to be a constant. Ref. [16] broken the orbit transfer problem into segments, which are determined more or less at random, and the GA is applied to solve the near-optimal solutions. Though control parameterization methods avoid the large number of optimization variables and the derivation of the analytical first-order necessary optimality conditions, the solution found is properly near-optimal, in the sense that it is the minimizing solution within the class of functions used to represent the control.

This paper focuses on the application of the PSO for fuel-optimal low-thrust formation flying trajectory optimization, the differences of the method are mainly in: 1) The PMP is used to derive the first-order necessary optimality conditions, which converts the continuous optimal control problem exactly into a parameter optimization problem in the initial costates. The control profile is determined by the costates indirectly, which would avoid the near-optimal solution when assuming constant thrust-pointing angle [15] or adopting the B-splines [5, 18, 19] or polynomial function [17] to parameterize the control profile; 2) The search space of the initial costates is determined based on the associated global fuel-optimal impulsive trajectory; 3) The control structure is not fixed a prior, but determined automatically. This could explore the possible control structures to obtain the global optimal solutions.

The remainder of this paper is organized as follows. In Sec. 2, the fuel-optimal low-thrust trajectory optimization problems are stated. The PSO is briefly reviewed in Sec. 3. In Sec. 4, Performance of the PSO is analyzed by simulating typical formation flying reconfiguration problems. Conclusions are drawn in Sec. 5.

2. Fuel-Optimal Low-Thrust Formation Trajectory Optimization Problems

2.1. Relative Dynamic Equations

Assuming that there are no orbital perturbations, the linear formation flying relative dynamics motion near circular reference orbit can be stated by the well-known Clohessy-Wiltshire equations [21], which are set up in the chief satellite's local-vertical-local horizontal (LVLH) frame. Denote ν as the chief's true anomaly, then, by taking ν as the independent variable, the relative motion of the deputy with respect to the chief in the chief's LVLH frame is given by

$$\begin{aligned} x'' - 3x - 2y' &= u_x \kappa \\ y'' + 2x' &= u_y \kappa \\ z'' + z &= u_z \kappa \end{aligned} \tag{1}$$

where x, y, and z are the radial, along track, and out-of-plane positions, respectively. u_x, u_y, and u_z are the components of the unit control direction; $(')$ denotes the derivative with respect to the chief's true anomaly; and $\kappa = T_{\max} / (mn^2)$ with m and n are, respectively, the deputy's mass and chief's orbital angular velocity; $T_{\max}$ is the maximum thrust magnitude.

Denote $\boldsymbol{x} = [x, y, z, x', y', z']^T$ and $\boldsymbol{u} = [u_x, u_y, u_z]^T$ as the state and control direction vectors, respectively. Equation (1) can be stated in a matrix form as

$$\boldsymbol{x}' = \boldsymbol{A}\boldsymbol{x} + \boldsymbol{B}\boldsymbol{u} \tag{2}$$

where the matrices $\boldsymbol{A}$ and $\boldsymbol{B}$ are given by

$$\boldsymbol{A} = \begin{bmatrix} 0 & 0 & 0 & 1 & 0 & 0 \\ 0 & 0 & 0 & 0 & 1 & 0 \\ 0 & 0 & 0 & 0 & 0 & 1 \\ 3 & 0 & 0 & 0 & 2 & 0 \\ 0 & 0 & 0 & -2 & 0 & 0 \\ 0 & 0 & -1 & 0 & 0 & 0 \end{bmatrix}, \quad \boldsymbol{B} = \begin{bmatrix} 0 & 0 & 0 \\ 0 & 0 & 0 \\ 0 & 0 & 0 \\ \kappa & 0 & 0 \\ 0 & \kappa & 0 \\ 0 & 0 & \kappa \end{bmatrix} \tag{3}$$

The homogeneous function of Eq. (2) has stable solutions. Two typical stable configurations considered in this paper are [21]

1) The general circular orbit (GCO). In the GCO, the deputy and chief satellites maintain a constant separation from each other. The formation is mathematically defined as $x^2 + y^2 + z^2 = \rho^2$, ρ is the formation radius. The position vector is given by

$$\begin{bmatrix} x \\ y \\ z \end{bmatrix} = \frac{\rho}{2} \begin{bmatrix} \sin(\nu + \alpha) \\ 2\cos(\nu + \alpha) \\ \sqrt{3}\sin(\nu + \alpha) \end{bmatrix} \tag{4}$$

2) The projected circular orbit (PCO). In the PCO, the deputy and chief maintain a fixed relative distance only on the y-z plane. The formation is mathematically defined as $y^2 + z^2 = \rho^2$. and the position vector is given by

$$\begin{bmatrix} x \\ y \\ z \end{bmatrix} = \frac{\rho}{2} \begin{bmatrix} \sin(\nu + \alpha) \\ 2\cos(\nu + \alpha) \\ 2\sin(\nu + \alpha) \end{bmatrix} \tag{5}$$

The low-thrust formation control problem can be stated as

$$\boldsymbol{x}_1 = \boldsymbol{\Phi}(\nu_1)\boldsymbol{\Phi}(\nu_0)^{-1}\boldsymbol{x}_0 + \boldsymbol{\Phi}(\nu_1)\int_{\nu_0}^{\nu_1} \boldsymbol{\Phi}(\nu)^{-1}\boldsymbol{B}\boldsymbol{u}\,\mathrm{d}\nu \tag{6}$$

where ν_0 and ν_1 are the initial and terminal true anomalies; $\boldsymbol{x}_0$ and $\boldsymbol{x}_1$ denote the initial and terminal states, respectively; $\boldsymbol{\Phi}(\nu)$ is a fundamental matrix solution associated with $\boldsymbol{A}$ and $\boldsymbol{\Phi}(\nu)^{-1}$ is the inverse matrix. The expression is given by

$$\mathbf{\Phi}(\nu)=\begin{bmatrix} \cos\nu & \sin\nu & 2 & 0 & 0 & 0 \\ -2\sin\nu & 2\cos\nu & -3\nu & 1 & 0 & 0 \\ 0 & 0 & 0 & 0 & \cos\nu & \sin\nu \\ -\sin\nu & \cos\nu & 0 & 0 & 0 & 0 \\ -2\cos\nu & -2\sin\nu & -3 & 0 & 0 & 0 \\ 0 & 0 & 0 & 0 & -\sin\nu & \cos\nu \end{bmatrix} \tag{7}$$

2.2. Fuel-Optimal Low-Thrust Control Problem

In this paper, two constraints on the control direct vector are considered

$$-1 \le u_k \le 1, k = x, y, z \tag{8}$$

$$\|\boldsymbol{u}\|_2 = \sqrt{u_x^2 + u_y^2 + u_z^2} \le 1 \tag{9}$$

Equation (8) implies the admissible control lies within a cube, while Eq. (9) implies the admissible control lies within a sphere. Then, the mass variation equation yields

$$m' = k_m \|\boldsymbol{u}\|_j,\ j = 1, 2 \tag{10}$$

where $k_m = -T_{\max}/(n v_e)$, $v_e = I_{sp} g_0$, $g_0 = 9.80665\text{ms}^{-2}$ is the gravitational acceleration; I_{sp} is the specific impulse; and $\|\cdot\|_j$ denotes the L^j norm of a vector.

The performance index of the fuel-optimal control problem that has to be minimized is

$$J = \int_{\nu_0}^{\nu_1} \|\boldsymbol{u}\|_j \, \mathrm{d}\nu,\ j = 1, 2 \tag{11}$$

where $j = 1$ is associated with the control constraint in Eq. (8) and $j = 2$ is associated with the control constraint in Eq. (9).

Define $\boldsymbol{\lambda} = [\lambda_x, \lambda_y, \lambda_z, \lambda_{x'}, \lambda_{y'}, \lambda_{z'}]^T$ and λ_m as the costates associated with $\boldsymbol{x}$ and m, respectively. In the view of the dynamic equations presented in Eqs. (2) and (10), the Hamiltonian function for the low-thrust trajectory optimization problem with the performance index in Eq. (11) is defined as

$$H = \|\boldsymbol{u}\|_j + \boldsymbol{\lambda}^T \boldsymbol{x}' + \lambda_m m' \tag{12}$$

By applying the PMP, the costates' differential equations yields

$$\boldsymbol{\lambda}' = -\boldsymbol{A}^T\boldsymbol{\lambda} \tag{13}$$

$$\lambda_m' = \frac{1}{m}\boldsymbol{\lambda}^T\boldsymbol{B}\boldsymbol{u} \tag{14}$$

The solution of $\boldsymbol{\lambda}$ is given by

$$\boldsymbol{\lambda} = \boldsymbol{\Phi}(\nu)^{-T}\boldsymbol{c} \tag{15}$$

where $\boldsymbol{c} \in \mathbb{R}^{6\times 1}$ is a nonzero constant vector to be determined.

Define $\boldsymbol{p} = [p_x, p_y, p_z]^T = \boldsymbol{B}^T\boldsymbol{\lambda}$ as the primer vector. By applying the PMP, the optimal control $\boldsymbol{u}^*$ of the fuel-optimal low-thrust FFTO problem for $j = 2$, denoted as $\mathcal{P}_2$, yields

$$\boldsymbol{u}^* = \begin{cases} -\sigma\dfrac{\boldsymbol{p}}{\|\boldsymbol{p}\|_2}, & \text{if } \|\boldsymbol{p}\|_2 \neq 0 \\ \boldsymbol{0}_{3\times 1}, & \text{if } \|\boldsymbol{p}\|_2 = 0 \end{cases} \tag{16}$$

where the thrust magnitude ratio σ is given by

$$\sigma = \begin{cases} 1, & \text{if } s < 0 \\ 0, & \text{if } s > 0 \\ \in [0,1], & \text{if } s = 0 \end{cases} \tag{17}$$

and s is the switching function, defined as

$$s = 1 + \lambda_m k_m - \|\boldsymbol{p}\|_2 \tag{18}$$

Define $b = 1 + \lambda_m k_m$, the optimal control $\boldsymbol{u}^*$ of the fuel-optimal low-thrust FFTO problem for $j = 1$, denoted as $\mathcal{P}_1$, yields

1) If $b > 0$

$$u_k^* = \begin{cases} -1, & \text{if } p_k > b \\ 1, & \text{if } p_k < -b \\ 0, & \text{if } p_k \in (-b, b) \\ u \in [-1, 0], & \text{if } p_k = b \\ u \in [\ 0, 1], & \text{if } p_k = -b \end{cases} \tag{19}$$

2) If $b = 0$

$$u_k^* = \begin{cases} -1, & \text{if } p_k > 0 \\ 1, & \text{if } p_k < 0 \\ u \in [0,1], & \text{if } p_k = 0 \end{cases} \tag{20}$$

3) If $b < 0$

$$u_k^* = \begin{cases} -1, & \text{if } p_k > 0 \\ 1, & \text{if } p_k < 0 \\ \in \{-1,1\}, & \text{if } p_k = 0 \end{cases} \tag{21}$$

Till now, the optimal controls for the fuel-optimal low-thrust FFTO problem under the two control direction constraints have been given. As can be seen, the optimal controls are completely determined by $\boldsymbol{\lambda}$ and λ_m that integrated from the given constant vector $\boldsymbol{c}$ and λ_{m0}. The terminal mass is left to be free, then terminal value of λ_m, denotes as λ_{m1}, must be zero. Let $\tilde{\boldsymbol{x}}_1$ denote the terminal state obtained by integrating the state-costate differential equations with the control $\boldsymbol{u}$ in Eq. (6) be replaced by $\boldsymbol{u}^*$. The optimal control problem has been reduced to find the initial costates that satisfy the following shooting function

$$S(\boldsymbol{c}, \lambda_{m0}) = [\tilde{\boldsymbol{x}}_1 - \boldsymbol{x}_1; \lambda_{m1}] = 0_{7\times1} \tag{22}$$

This is a typical TPBVP and several existing difficulties make the solution of the TPBVP formidable to obtain.

1) The shooting function may not be defined everywhere, and may be singular or non-differentiable at some points. The convergence theorems for Newton's method require the equations to be twice continuously differentiable and require their Jacobian matrix to be non-singular in the vicinity of the solution. Newton's method often fails to converge in the case of non-smooth equations.

2) The optimal control assumes the "on-off" form. The switching number and switching dates, which are completely problem dependent, are not known a prior and only can be determined when the optimal solutions have been found.

3) The shooting function is very sensitive to the initial costates. However, the costates have non-physical interpretations; it is very nonintuitive to estimate.

2.3. Framework of the solution method

To overcome the difficulties, the EAs are applied to solve the initial costates that satisfy the shooting function. EAs are heuristic based optimization methods and no gradient information is needed. Thus, the singularity or non-differentiability of the shooting function at some points will have no affection. The “ode45” integrator of MATLAB with its “events” function is adopted to propagate the trajectory and automatically detect the switching times according to the switching function, see Eqs. (16-21), and this would avoid a prior assumption of the control structure.

In designing the optimal trajectory, the computational cost mainly comes from 1) a relatively high cost in trajectory propagation (simulation of a trajectory) and 2) the number of trajectories that have to be iterated in finding the optimal solution [20]. Note that, the costate $\boldsymbol{\lambda}$ has analytical expression and is independent with $\boldsymbol{x}$, m, and λ_m, see Eq. (15) , thus only the differential equations of $\boldsymbol{x}$, m , and λ_m need to be propagated during the optimization. For the optimization of the EAs, the number of the trajectories propagated is large. Then, combining this property into the trajectory propagation would reduce nearly 50% of the computational cost. For problem $\mathcal{P}_2$, the trajectory propagation algorithm is given in Fig. 1. For problem $\mathcal{P}_1$, the trajectory propagation algorithm is almost the same and is not given; only pay attention to the differences of the optimal controls in Eqs. (19-21)

Set the initial conditions $\nu_T = \nu_0$ and $\boldsymbol{X}(\nu_0) = [\boldsymbol{x}_0; m_0; \lambda_{m0}]$.
If $s(\nu_0) < 0$, **then** set $flag = -1$; **else** set $flag = 1$.
Do
    If $flag == -1$, **then** set $flag = 0$. (thrust arc)
        Integrate $\boldsymbol{X}(\nu)$ on $[\nu_T, \nu_1]$ to find ν that satisfies
        $|s(\nu)| < \varepsilon, \nu \in (\nu_T, \nu_1)$, and set $flag = 1$, $\nu_T = \nu$.
    If $flag == 1$, **then** set $flag = 0, \lambda_m' = m' = 0$. (coast arc)
        Analytically propagate $\boldsymbol{x}, \boldsymbol{\lambda}$ to ν that satisfies
        $|s(\nu)| < \varepsilon, \nu \in (\nu_T, \nu_1)$, and set $flag = -1$, $\nu_T = \nu$.
    If $flag == 0$, **then** the terminal states are obtained,
        i.e., $\boldsymbol{X}(\nu_1) = [\tilde{\boldsymbol{x}}_1; m_1; \lambda_{m1}]$. **Break**.
End Do (ε is the precision tolerance.)

Figure 1. Trajectory Propagation Algorithm

3. Particle Swarm Optimization for the Low-Thrust FFTO

3.1. Particle Swarm Optimization

PSO is a population-based stochastic optimization technique, inspired by the social behavior of bird flocking or fish schooling [10]. With some abuse of notation, let $\boldsymbol{\chi}_{j,G}$ denote the j th particle of the G generation when searching in a D-dimensional hyperspace, i.e., $\boldsymbol{\chi}_{j,G} = \{\boldsymbol{c}, \lambda_{m0}\}_{j,G}$. It is associated with a velocity vector $\boldsymbol{v}_{j,G}$. Suppose each particle “remembers” its historical best position $\boldsymbol{\chi}_{j_B,G}$ and “knows” the best position $\chi_{B,G}$ ever visited by the entire swarm. Then the position and velocity vectors are iteratively updated according to

$$\boldsymbol{v}_{j,G+1} = c_I \boldsymbol{v}_{j,G} + c_C \left(\boldsymbol{\chi}_{j_B,G} - \boldsymbol{\chi}_{j,G} \right) + c_S \left(\boldsymbol{\chi}_{B,G} - \boldsymbol{\chi}_{j,G} \right) \tag{23}$$

$$\boldsymbol{\chi}_{j,G+1} = \boldsymbol{\chi}_{j,G} + \boldsymbol{v}_{j,G+1} \tag{24}$$

where c_I , c_C , and c_S are called the initial, cognitive, and social (stochastic) scaling factors, respectively. Their expressions are given by [14]

$$c_I = \frac{1 + r_1(0,1)}{2}, c_C = 1.49445 r_2(0,1), c_S = 1.49445 r_3(0,1) \tag{25}$$

where $r_1(0,1)$, $r_2(0,1)$, and $r_3(0,1)$ represent three independent random numbers with uniform distribution between 0 and 1. The particles' velocities are limited to a fixed low-upper bound, that equal to one-quarter of the respective positions' variation range [23].

In this paper, the initial costates of the impulsive optimal solution of the FFTO problem are enlarged to determine the search space of the particle's position vector.

3.2. Handling of the Shooting Function Constraint

EAs always perform unconstrained search. When solving constrained optimization problems, they require additional mechanisms to handle constraints. Constrained optimization problems are generally more difficult to solve than unconstrained ones. Constraint handling methods can be found in Refs. [24] and [25].

Since the initial costates are used as the decision variables, the equality constraints of the shooting function have no direct effect on the search space. Meanwhile, the associated global optimal impulsive solution can provide a reasonable search space that guarantees the convergence. Then, to handle the equality constraints in the shooting function, in this paper, a penalty modified performance index is adopted

$$\tilde{J}(\boldsymbol{\chi}_{j,G}) = J(\boldsymbol{\chi}_{j,G}) + p(\boldsymbol{\chi}_{j,G}) \tag{26}$$

The penalty function $p(\boldsymbol{\chi}_{j,G})$ in Eq. (26) is defined as

$$p(\boldsymbol{\chi}_{j,G}) = \left\| S(\boldsymbol{\chi}_{j,G}) \right\|_2 \tag{27}$$

In this paper, the units of position is in "km" and units of velocity is in "km/rad". Then, when $p(\boldsymbol{\chi}_{j,G}) \to 0.001$, the position violation approaches 1 m and velocity violation approaches 1 mm/s.

However, PSO may suffer the defect of convergence speed and accuracy because the heuristic mechanism, especially when the objective function is very sensitive to the initial costates. Thus, to speed the convergence of the PSO, the nonlinear solver HYBRD/HYBRJ is adopted to perform a local search for the particle that satisfies $p_M - p(\chi_{B,G}) \le 0.02$ and $p(\chi_{B,G}) \le 0.5$, where p_M denotes the mean penalty of the current generation.

4. Numerical Examples

The GCO to PCO reconfiguration problem is considered. The deputy's initial mass is $m_0 = 50$ kg. The thruster parameters are $T_{\max} = 0.1$ N, I_{sp} =1000 s. The initial and terminal true anomalies are $\nu_0 = 0$ and $\nu_1 = 2\pi$. The deputy's initial state on the GCO is $\boldsymbol{x}_0 = [-0,1,0,0.5,0,\sqrt{3}/2]^T$; the terminal state on the PCO is $\boldsymbol{x}_1 = [-0,2,0,1,0,2]^T$.

For the $\mathcal{P}_2$ problem, the fuel optimal impulsive and low-thrust reconfiguration trajectories are depicted in Fig. 2. Variation ranges of the decision variables are set as $\boldsymbol{c} \in 2[-\|\tilde{\boldsymbol{c}}\|,\|\tilde{\boldsymbol{c}}\|]$, $\lambda_{m0} \in [0,1]$, $\tilde{\boldsymbol{c}}$ is the impulsive results. The initial costates for the impulsive and low-thrust trajectories are presented in Table 1. The results gained are almost the same as using the homotopic approach in Ref. [22]. Compared with Ref. [22], the method in this paper is much more simple and direct. However, the counterpart is that the computational cost is relatively higher. Time history of $p_M - p(\chi_{B,G})$ during the PSO optimization is depicted in Fig. 3.

Table 1. Costates for the Impulsive and Low-Thrust Trajectories for $\mathcal{P}_2$

Trajectories	Nonzero Constant Vector $\boldsymbol{c}$	λ_{m0}
$\mathcal{P}_2$, Imp.*	[7.53e-16;-0.403442;-1.48e-15;-4.09e-18;-1.19e-18;-0.915005]	×
$\mathcal{P}_2$, Low*	[-0.062523;0.003317;8.664e-7;-0.227678;-0.031262;-0.516624]	0.013928

Imp.* refers to the impulsive trajectory and Low* refers to the low-thrust trajectory.

For the $\mathcal{P}_1$ problem, the fuel-optimal impulsive and low-thrust reconfiguration trajectories are depicted in Fig. 4. The fuel-optimal impulsive and low-thrust trajectories are almost the same, the differences shown in Fig. 4 are tiny. Simulation results found that, using the PSO directly to find the optimal $\boldsymbol{c}$ that satisfies the shooting function is difficult and the PSO may not be able to converge to a suitable value that for the HYBRD/HYBRJ optimizer. Meanwhile, as the impulse number, directions, and axes can be determined easily from the PSO, then the "fmincon" function of MATLAB can be used to optimize the thrust times of each thrust arc. The initial estimated thrust times are gained from the Ziolkovsky formula. The results of the fuel-optimal impulsive and low-thrust reconfiguration trajectories are given in Tables 2-4, respectively. In Tables 2-4, the negative sign means that the corresponding impulse is applied along the negative impulse axis.

Note that, for the $\mathcal{P}_1$ problem, the z direction motion and impulses are both independent from the xy plane motion and impulses. Thus, analytical solutions exist and the z direction impulses can be applied when $z=0$. For the reconfiguration problem considered in this paper, the z direction impulses can be divided into seven cases as given in Table 3, where $k \in [0,1]$ and $a,b,c \in [0,1]$, $a+b+c=1$. In Table 4, the 7th case of the z-plane is adopted; by setting $k=0.5, a=c=0.25, b=0.5$ and use the resulting impulse magnitude to estimate the thrusting times.

Table 2. Fuel-Optimal Impulsive Reconfiguration of the xy-plane for $\mathcal{P}_1$

Impulse Number	Impulse Time	Axis	Impulse Magnitude
1	0	y	0.055103
2	1.789776	y	-0.128058
3	4.493409	y	0.128058
4	2π	y	-0.055103

Table 3. Fuel-Optimal Impulsive Reconfiguration of the z-plane for $\mathcal{P}_1$

Cases	Impulse Time	Axis	Impulse Magnitude
1	0	z	1.133974
2	π	z	-1.133974
3	2π	z	1.133974
4	$\{0, \pi\}$	z	$\{1.133974k, -1.133974(1-k)\}$
5	$\{0, 2\pi\}$	z	$\{1.133974k, 1.133974(1-k)\}$
6	$\{\pi, 2\pi\}$	z	$\{-1.133974k, 1.133974(1-k)\}$
7	$\{0, \pi, 2\pi\}$	z	$\{1.133974a, -1.133974b, 1.133974c\}$

Table 4. Fuel-Optimal Low-Thrust Reconfiguration Results for $\mathcal{P}_1$

Thrust Arc	Axis	Thrust Arc Times
1	y	[0, 0.030921]
2	$-y$	[1.762363, 1.834317]
3	y	[4.448880, 4.520828]
4	$-y$	[6.252274, 2π]
5	z	[0, 0.158526]
6	$-z$	[2.983091, 3.300115]
7	z	[6.124687, 2π]

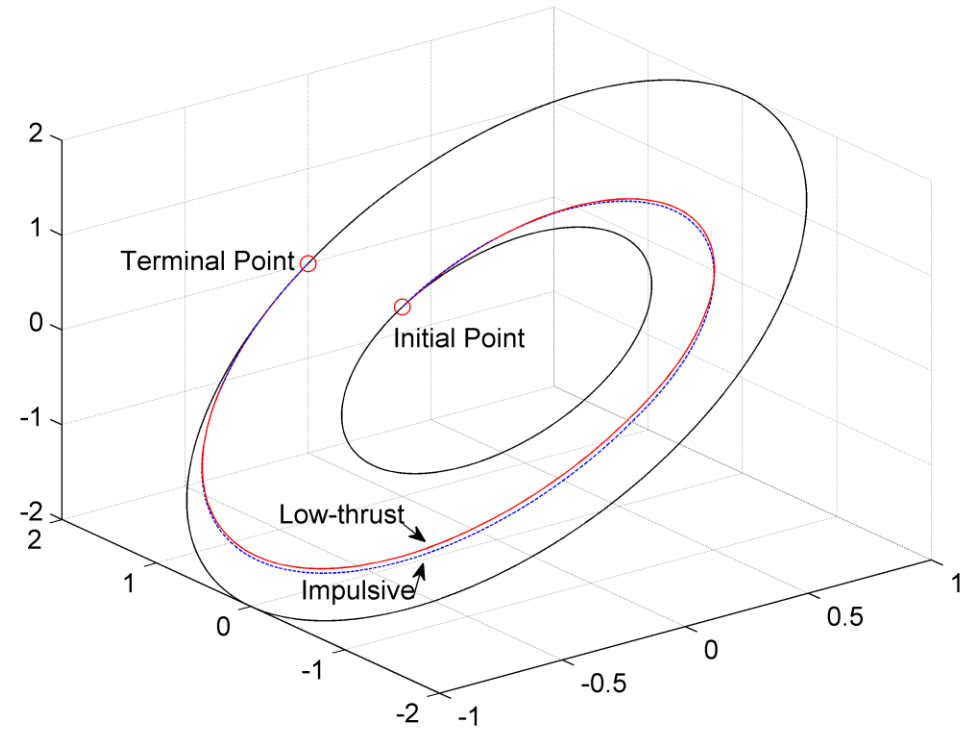

Figure 2. Fuel-Optimal Reconfiguration Trajectories for $\mathcal{P}_2$

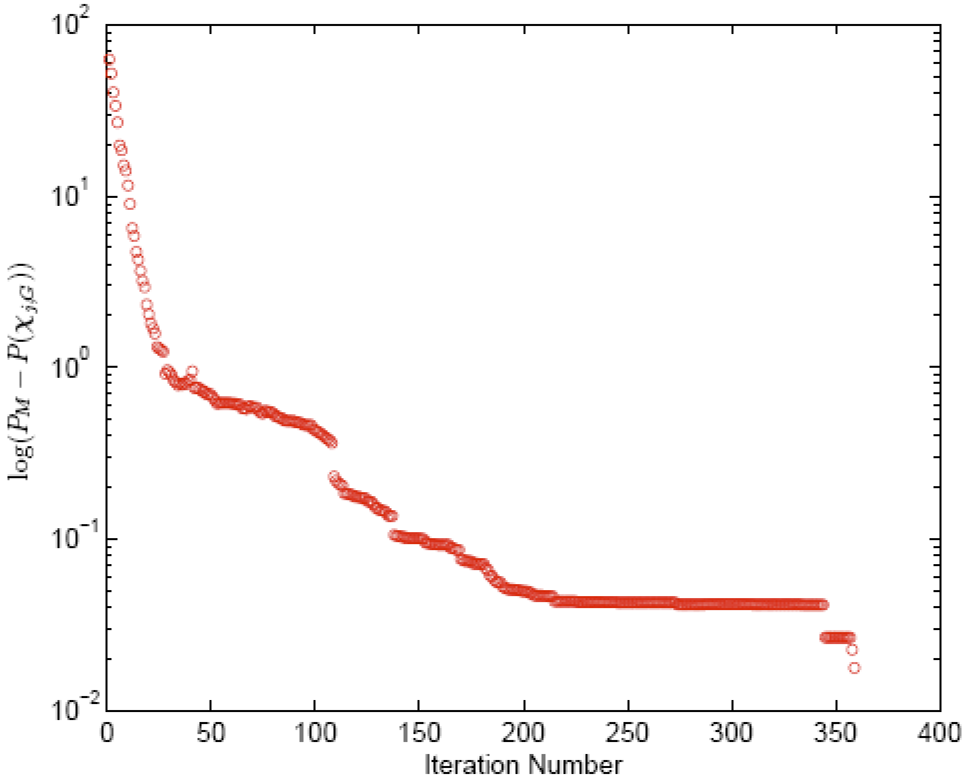

Figure 3. Time History of the Penalty Function for $\mathcal{P}_2$

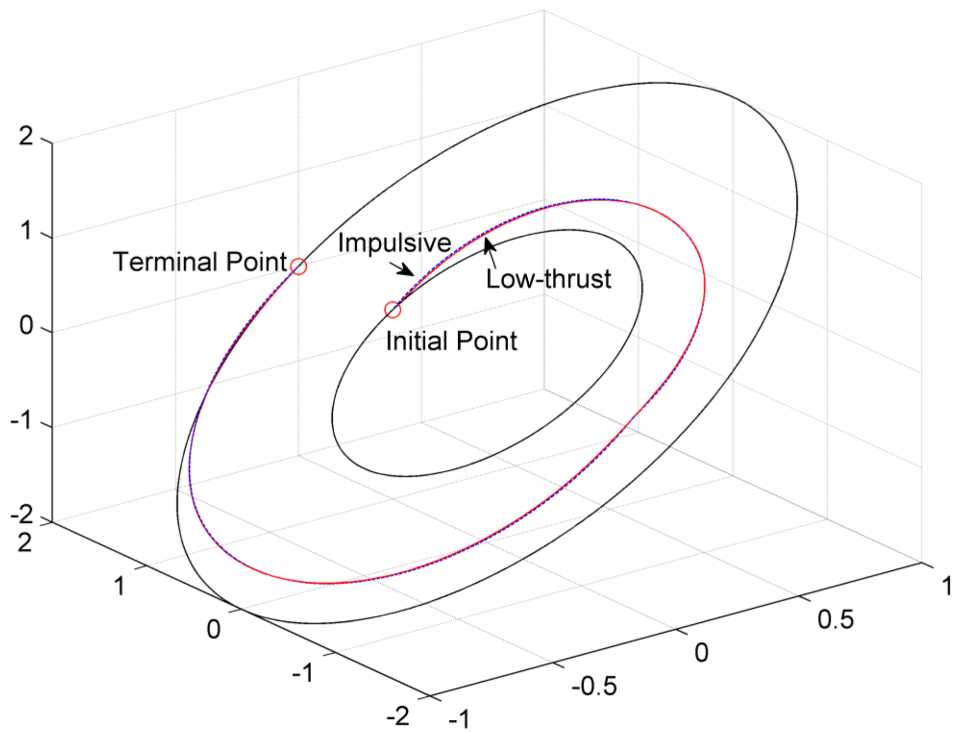

Figure 4. Fuel-Optimal Reconfiguration Trajectories for $\mathcal{P}_1$

5. Conclusions

In this paper, the particle swarm optimization technique was used to obtain the fuel-optimal low-thrust reconfiguration trajectories for formation-flying satellites. Numerical examples found that fuel-optimal impulsive solutions can provide a suitable search space of the initial costates. In the general cases, for the control direction within a sphere, simulation results also shown that the PSO can not converge to an accurate solution that satisfies the shooting function. The probably reasons are that, the shooting function is very sensitive and the magnitudes of the initial costates are quit different from each other. However, the PSO can always converge to a suitable solution, with which the HYBRD/HYBRJ optimizer could converge to the optimal solution accurately and quickly.

6. References

[1] Scharf, D. P., Hadaegh, F. Y., and Ploen, S. R., “A Survey of Spacecraft Formation Flying Guidance and Control (Part I): Guidance”, Proceeding of the American Control Conference, IEEE Publications, Piscataway, NJ, Vol. 4, 2003, pp. 1733-1739.

[2] Scharf, D. P., Hadaegh, F. Y., and Ploen, S. R., “A Survey of Spacecraft Formation Flying Guidance and Control (Part II): Control”, Proceeding of the American Control Conference, IEEE Publications, Piscataway, NJ, Vol. 4, 2004, pp. 2976-2985.

[3] Massari, M., and Zazzera, F. B., “Optimization of Low-Thrust Reconfiguration Maneuvers for Spacecraft Flying in Formation”, Journal of Guidance, Control, and Dynamics, Vol. 32, No. 5, 2009, pp. 1629-1638.

[4] Betts, J. T., “Survey of Numerical Methods for Trajectory Optimization”, Journal of Guidance, Control, and Dynamics, Vol. 21, No. 2, 1998, pp. 193-207.

[5] Conway, B. A., “A Survey of Methods Available for the Numerical Optimization of Continuous Dynamics Systems”, Journal of Optimization Theory and Applications, Vol. 152, No. 2, 2012, pp. 271-306.

[6] Bryson, A. E., and Ho, Y.-C., Applied Optimal Control, Hemisphere, Washington, D.C., 1975, pp. 214-215, 246-262.

[7] Goldberg, D. E., “Genetic Algorithms in Search, Optimization, and Machine Learning”, Addison Wesley, Boston, 1989, pp. 1-54.

[8] Storn, R., Price, K., “Differential Evolution: A Simple and Efficient Adaptive Scheme for Global Optimization over Continuous Spaces”, International Computer Science Inst., TR 95-012, Berkeley, CA, 1995.

[9] Swagatam, D., Ponnuthurai, N. S., “Differential evolution: a survey of the state-of-the-art”, IEEE transactions on evolutionary computation, Vol. 15, No. 1, 2011, pp. 4-31.

[10] Kennedy, J., Eberhart, R., “Particle swarm optimization”, Proceedings of the IEEE international conference on neural networks. IEEE Publication, Piscataway, NJ, 1995, pp. 1942-1948.

[11] Ploi, R., Kennedy, J., Blackwell, T., “Particle swarm optimization, an overview”, Swarm Intelligence, Vol. 1, 2007, pp. 33-57.

[12] Bessette, C. R., Spencer, D. B., “Identifying Optimal Interplanetary Trajectories through a Genetic Approach”, AIAA/AAS Astrodynamics Specialist Conference and Exhibit, Keystone, CO, AIAA Paper 20066306.

[13] Sentinella, M. R., Casalino, L., “Cooperative Evolutionary Algorithm for Space Trajectory Optimization”, Celestial Mechanics and Dynamical Astronomy, Vol. 105, No. 1-3, 2009, pp. 211-217.

[14] Pontani, M., Conway, B. A., “Particle swarm optimization applied to impulsive orbital transfers”, Acta Astronautica, Vol. 74, 2012, pp. 141-155.

[15] Rauwolf, G., Coverstone-Carroll, V., “Near-Optimal Low-Thrust Orbit Transfers Generated by a Genetic Algorithm”, Journal of Spacecraft and Rockets, Vol. 33, No. 6, 1996, pp. 859-862.

[16] Wall, B. J., Conway, B. A., "Near-Optimal Low-Thrust Earth-Mars Trajectories Found Via a Genetic Algorithm", Journal of Guidance, Control, and Dynamics, Vol. 28, No. 5, 2005, pp. 1027-1031.

[17] Pontani, M., Conway, B. A., "Particle Swarm Optimization Applied to Space Trajectories", Journal of Guidance, Control, and Dynamics, Vol. 35, No. 5, 2010, pp. 1429-1441.

[18] Ghosh, P., Conway, B. A., "Numerical Trajectory Optimization with Swarm Intelligence and Dynamic Assignment of Solution Structure", Journal of Guidance, Control, and Dynamics, Vol. 35, No. 4, 2012, pp. 1178-1191.

[19] Pontani, M., Ghosh, P. Conway, B. A., "Particle Swarm Optimization of Multiple-Burn Rendezvous Trajectories", Journal of Guidance, Control, and Dynamics, Vol. 35, No. 4, 2012, pp. 1192-1207.

[20] Betts, J. T., Huffman, W. P., "Trajectory Optimization on a Parallel Processor", Journal of Guidance, Control, and Dynamics, Vol. 14, No. 2, 1991, pp. 431-439.

[21] Alfriend, K. T., Vadali, S. R., Gurfil, P., How, J. P., and Breger, L. S., "Spacecraft Formation Flying: Dynamics, Control and Navigation", 1st ed., Elsevier Astrodynamics Series, Butterworth-Heinemann, Kidlington, U. K., 2010, pp. 59-64.

[22] Li, J., Xi, X., "Fuel-Optimal Low-Thrust Reconfiguration of Formation Flying Satellites via Homotopic Approach", Journal of Guidance, Control, and Dynamics, Vol. 35, No. 6, 2012, pp. 1192-1207.

[23] Sentinella, M. R., Casalino, L., "Hybrid Evolutionary Algorithm for the Optimization of Interplanetary Trajectories", Journal of Guidance, Control, and Dynamics, Vol. 35, No. 4, 2012, pp. 1178-1191.

[24] Coello, C. A. C., "Theoretical and Numerical Constraint-Handling Techniques Used with Evolutionary Algorithms: A Survey of the State-of-the-Art," Comput. Methods Appl. Mech. Eng., Vol. 191, No. 11-12, 2002, pp. 1245-1287.

[25] Michalewicz, Z., Schoenauer, M., "Evolutionary Algorithms for Constrained Parameter Optimization Problem," Vol. 4, No. 1, 1996, pp. 1-32.

[26] Farmani, R., Wright, J. A., "Self-Adaptive Fitness Formulation for Constrained Optimization," IEEE Transaction on Evolutionary Computation, Vol. 7, No. 5, 2003, pp. 445-455.

[27] Tessema, B., Yen, G. G., "A Self-Adaptive Penalty Function Based Algorithm for Constrained Optimization," Proceeding of IEEE Congr. Evol. Comput., Vancouver, BC, Canada, 2006, pp. 246-253.